Journal of Sound and Vibration (1997) **208**(3), 407–426

STATISTICAL ENERGY ANALYSIS OF PERIODICALLY STIFFENED DAMPED PLATE STRUCTURES

R. S. Langley and J. R. D. Smith

Department of Aeronautics and Astronautics

and

F. J. Fahy

Institute of Sound and Vibration Research, University of Southampton, Southampton SO17 1BJ, England

(*Received* 6 *March* 1997, *and in final form* 10 *June* 1997)

Stiffened panels are used widely in aerospace and marine vehicles, and it is often necessary to predict high frequency noise and vibration levels in structures of this type. The present work is concerned with modelling high frequency vibration transmission through a stiffened panel within the context of Statistical Energy Analysis (SEA). It is proposed that the panel can be modelled as a damped coupling element between two adjoining structural components, and the transmission and absorption coefficients calculated on the basis of periodic structure theory. The method is applied to the forced response of two panels which are coupled by a stiffened panel and a comparison is made with (i) exact results obtained by using the dynamic stiffness method, (ii) results yielded by a conventional SEA approach, and (iii) results yielded by wave intensity analysis (WIA). The method is found to yield accurate response predictions which are a significant improvement upon the conventional SEA and WIA results obtained for the example system. Previous work has shown that vibration transmission through a periodic system can be very sensitive to structural disorder, and the present study includes an investigation of the effects of disorder in the stiffener spacing.

1. INTRODUCTION

Many types of engineering structure are subjected to high frequency excitation, in the sense that the induced response has a vibrational wavelength which is small in comparison to the overall system dimensions. Typical examples include the response produced in a turbo-prop aircraft such as the Fokker F50 at the harmonics of the blade passing frequency (approximately multiples of 100 Hz), and the vibration levels induced on board a ship by the engines and the propeller, where cavitation noise can extend beyond 500 Hz. The short wavelength of the structural response leads to severe analytical difficulties in attempting to predict the system vibration levels at the design stage: for example, the conventional finite element method typically requires the use of around four elements per half wavelength of deformation, and this generally leads to models which are of a computationally impracticable size at high frequencies.

Much research effort has been devoted to the development of alternative analysis techniques which are capable of predicting high frequency vibration levels, and the most well known alternative approach is perhaps Statistical Energy Analysis (SEA) [1]. In SEA

0022–460X/97/480407 + 20 $25.00/0/sv971150

no attempt is made to recover the detailed displacement pattern of the structure, but rather the structure is modelled as an assembly of "subsystems" and the aim is to predict the vibrational energy level of each subsystem. This is done by establishing a set of power balance equations which are based on the key assumption that the energy flow between two connected subsystems is proportional to the difference in the subsystem modal energies. While SEA has been applied with considerable success to a wide range of structures, there is a continuing debate over the theoretical validity of the method (see, for example, references [2–4]), and it is true to say that the method yields very poor results for certain types of structure. One practical difficulty associated with the application of the method to aerospace and marine vehicles arises from the widespread use of stiffened plating in these structures; as yet there is no clear guideline as to how such plating is best incorporated within an SEA model, and this issue is discussed in what follows.

The present study is concerned with vibration transmission through a plate which is stiffened by a series of parallel stiffeners which are (nominally) evenly spaced. This situation can be likened to vibration transmission along an aircraft fuselage or a section of a ship hull, with the present stiffeners taking on the role of the structural frames. It is often argued that a stiffened plate can be modelled to a reasonable degree of accuracy by "smearing" the stiffener properties to produce an equivalent orthotropic plate. However, such an approach can be expected to be successful only if (i) the half wavelength of the panel vibration exceeds the stiffener spacing, and (ii) the stiffeners are sufficiently weak in bending relative to the plate bending stiffness. Condition (ii) depends to some extent upon the boundary conditions which are imposed on the panel edges—a stiffened panel which is simply supported on the edges parallel to the stiffeners and free on the other two edges will tend to have lower modes of vibration which are reasonably well predicted by a smeared model. However, if the panel is simply supported on all four sides then "rigid body" motion of the stiffeners will be restrained, and the stiffener bending stiffness will have a crucial influence on the nature of the lower modes of vibration. For aerospace and marine vehicles the frames are relatively stiff, and certainly at higher frequencies the conditions required for the successful application of the smearing approach will not be met.

In SEA terms, the other extreme to a "smeared" model of a stiffened plate would be to model each inter-stiffener plate element as a subsystem (or, more generally, as three subsystems to allow for the three types of wave motion which can occur in a flat plate). With this approach, the stiffeners act as coupling elements between the SEA subsystems, and the associated coupling loss factors can be found by considering wave transmission across a stiffener [5]. This general modelling approach has been applied with great success to box-type structures by Heron [6], although in that case the structure did not contain stiffened plates—rather, the stiffeners were used to assemble a set of relatively large panels. When applied to a stiffened plate this type of approach could face three potential difficulties: (i) the mode count in each plate element may be insufficient to justify inclusion as a separate SEA subsystem; (ii) the method could lead to a very large SEA model for a complete vehicle; and (iii) the method cannot capture any "periodic structure" type behaviour of the stiffened panel. Point (iii) is related to the fact that a periodically stiffened structure has very distinctive vibration characteristics, as outlined in what follows.

A periodic structure is defined as a structure that is composed of a number of identical units which are connected in a regular pattern. The stiffened plate structure considered in the present work forms a one-dimensional periodic structure, in which the basic unit consists of an inter-stiffener plate element with an attached stiffener. It is well known that wave motion through a structure of this type can occur only within certain frequency intervals known as pass bands; the pass bands are separated by stop bands in which propagating wave motion cannot occur. The incorporation of this type of behaviour within

an SEA model has received little attention other than in the work of Keane and Price [7] who considered two coupled periodic rod structures. Each rod structure was modelled as an SEA subsystem in which the modal density was calculated on the basis of periodic structure theory, it being noted that the natural frequencies of a periodic structure tend to lie within the pass bands. While this approach led to excellent results for the structure considered, it would appear to be difficult to extend the methodology to more general situations—not in terms of the validity of the method, but rather in terms of the practical calculation of the coefficients which appear in the SEA equations. For this reason a quite different approach is used here to model the stiffened plate: the plate is modelled as a *non-conservative coupling element* between different parts of the structure. Specifically, a three-part structure is considered, in which the middle plate is stiffened. The two outer plates are modelled as conventional SEA subsystems, while the middle plate is considered to act as a coupling element. The properties of this coupling element are calculated on the basis of periodic structure theory, and in this regard use is made of recent results concerning the band-averaged transmission coefficient of a periodic structure [8]. There has been much debate as to how the energy loss associated with a non-conservative coupling should be modelled within the context of SEA [9–11], and this issue is dealt with in the present work simply by using the absorption coefficient of the coupling element to make an appropriate addition to the loss factors of the adjoining elements. The general theory behind this approach is outlined in section 2, while the absorption and transmission coefficients associated with the stiffened plate are derived in section 3. A number of example applications are presented in section 4, where a comparison is made with exact results derived by using the dynamic stiffness method [12]. It is found that the present approach leads to an accurate prediction of the vibration transmission through the panel, while the conventional SEA approach (based on the modelling each inter-stiffener panel as a subsystem) can lead to a severe underestimate of the transmitted power. It is shown that the SEA results can be significantly improved by allowing for the wave filtering effect of the stiffeners by using a technique known as Wave Intensity Analysis [13], and the effect of structural disorder on the transmitted power is also considered in this section. Finally, the practical implications of the present work are discussed in section 5.

2. SEA MODELLING OF NON-CONSERVATIVELY COUPLED SUBSYSTEMS

A schematic of two two-dimensional subsystems which are coupled along an edge is shown in Figure 1. In the present context, the two subsystems represent unstiffened plates, while the coupling represents a stiffened plate which both transmits and dissipates energy.

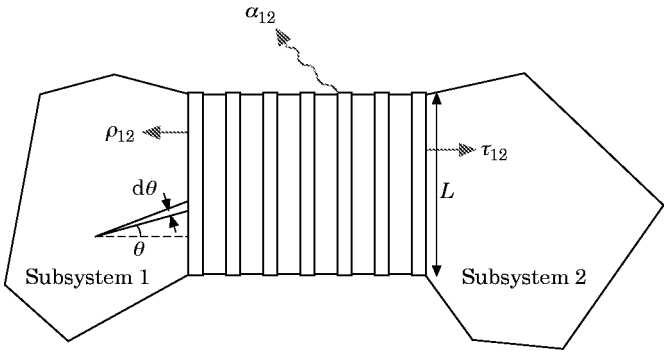

Figure 1. A schematic of the two-subsystem SEA model.

For the purposes of the present argument, the stiffened plate is assumed to have symmetric stiffeners so that only the bending motion of each plate need be considered.

An SEA model of the system shown in Figure 1 can be derived by considering energy flow across the coupling, and this is most easily done by considering the transmission of elastic wave motion. If the time averaged vibrational energy in subsystem 1 is represented by E_1, then the energy density can be written as E_1/A_1, where A_1 is the area of the subsystem. Now if it is assumed that the wave motion in the subsystem is "diffuse" so that the energy flow is evenly spread among all directions, then the energy flow associated with the angular range θ to $\theta + \mathrm{d}\theta$ can be written as $c_{g1}\,(E_1/A_1)\,(\mathrm{d}\theta/2\pi)$, where c_{g1} is the wave group velocity. This is strictly the energy flow per unit length measured along the wave crest, so that the power incident on the coupling is $c_{g1}\,(E_1/A_1)\,(\mathrm{d}\theta/2\pi)L\cos\theta$, where L is the length of the coupled edge. Now part of this power is transmitted to subsystem 2 and part is dissipated within the coupling, with the remainder being reflected back into subsystem 1. The fraction of power which is transmitted is given by the *transmission coefficient* $\tau_{12}\,(\theta)$, while the fraction absorbed is given by the *absorption coefficient* $\alpha_{12}\,(\theta)$. The total power lost through the coupling can thus be written as

$$P_{loss} = \int_{-\pi/2}^{\pi/2} [\tau_{12}\,(\theta) + \alpha_{12}\,(\theta)]\,(E_1\,c_{g1}\,L/2\pi A_1)\cos\theta\,\mathrm{d}\theta = [\langle\tau_{12}\rangle + \langle\alpha_{12}\rangle]E_1\,c_{g1}\,L/\pi A_1), \quad (1)$$

where the diffuse field transmission and absorption coefficients $\langle\tau_{12}\rangle$ and $\langle\alpha_{12}\rangle$ are defined as

$$\langle\tau_{12}\rangle = \tfrac{1}{2}\int_{-\pi/2}^{\pi/2} \tau_{12}\,(\theta)\cos\theta\,\mathrm{d}\theta, \qquad \langle\alpha_{12}\rangle = \tfrac{1}{2}\int_{-\pi/2}^{\pi/2} \alpha_{12}\,(\theta)\cos\theta\,\mathrm{d}\theta. \quad (2, 3)$$

Now subsystem 1 will also gain power through the junction from subsystem 2. By analogy with equation (1), this power can be written in the form

$$P_{gain} = \langle\tau_{21}\rangle(E_2\,c_{g2}\,L/\pi A_2). \quad (4)$$

The total power balance equation for subsystem 1 then takes the form

$$\omega\eta_1\,E_1 + P_{loss} - P_{gain} = P_1, \quad (5)$$

where the first term on the left is the power dissipated internally (η_1 being the loss factor), and the term on the right is the power input from external sources. Equations (1)–(5) can be combined to yield the power balance equation in the standard SEA format [1],

$$\omega\eta_{1\mathrm{eff}}\,E_1 + \omega\eta_{12}\,v_1\,(E_1/v_1 - E_2/v_2) = P_1, \quad (6)$$

where

$$v_i = \omega A_i/(2\pi c_i\,c_{gi}), \qquad \eta_{12} = c_{g1}\,L\langle\tau_{12}\rangle/(\pi\omega A_1), \qquad \eta_{1\,\mathrm{eff}} = \eta_1 + \eta_{12}\langle\alpha_{12}\rangle/\langle\tau_{12}\rangle. \quad (7\text{–}9)$$

Here v_i is the modal density of subsystem i (c_i is the phase speed), and η_{12} is the coupling loss factor. It should be noted that in deriving equation (6) the reciprocity relation $\langle\tau_{12}\rangle/c_1 = \langle\tau_{21}\rangle/c_2$ has been employed. The power balance equation for subsystem 2 has precisely the form of equation (6) with the subscripts 1 and 2 interchanged.

It has been shown in this section that under the normal "diffuse wave" set of assumptions, the basic form of the SEA equations is unchanged by the presence of dissipation in a coupling element. The only detailed changes are that (i) the transmission

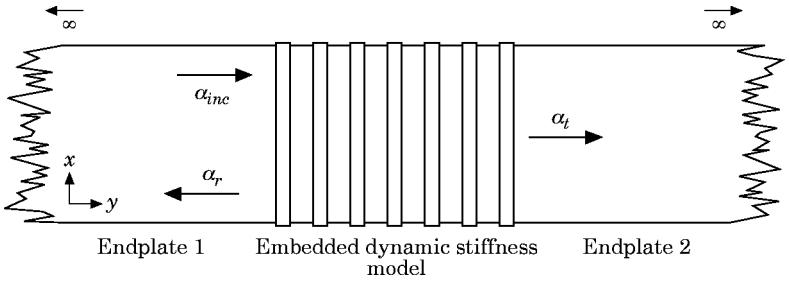

Figure 2. A schematic of the transmission model.

coefficient used in the coupling loss factor is that which arises in the presence of dissipation, and (ii) an appropriate addition must be made to the subsystem loss factors to account for absorption by the junction. The latter point is consistent with the findings of Beshara and Keane [11] regarding the appropriate form of the SEA equations for non-conservatively coupled subsystems. Furthermore, equation (9) is analogous to the subsystem loss factor employed by Craik [14] to allow for boundary absorption effects.

The transmission and absorption coefficients which are associated with a periodically stiffened plate element are derived in the following section.

3. TRANSMISSION AND ABSORPTION COEFFICIENTS

As mentioned in the Introduction, the present concern is with vibration transmission through a stiffened panel, and a schematic of the system under investigation is shown in Figure 2. In order to apply the analysis of section 2 to this structure it is necessary to compute the transmission and absorption coefficients $\langle \tau_{12} \rangle$ and $\langle \alpha_{12} \rangle$ of the stiffened panel, and two methods of doing this are outlined in the present section. The first approach is an exact calculation in which the transmission through an M-bay stiffened panel is analysed by using a variant of the dynamic stiffness method [12]. In order to facilitate this calculation it is assumed that the stiffened panel is simply supported along the two longitudinal edges, and the stiffeners are taken to be symmetric, so that there is no coupling between the in-plane and out-of-plane motion of the plate. The second method of calculating $\langle \tau_{12} \rangle$ and $\langle \alpha_{12} \rangle$ is an approximate and computationally efficient technique which is based on the one-dimensional waveguide theory developed in reference [8]; with this approach it is only necessary to calculate the wave transmission coefficient of a single plate/stiffener junction.

3.1. EXACT CALCULATION

The fact that the structure shown in Figure 2 is simply supported along the longitudinal edges implies that the out-of-plane displacement may be expressed as a Fourier series involving terms proportional to $\sin(n\pi x/b)$, where n is an integer and b is the panel width. For each value of n, bending wave transmission through the system can be analyzed by using a variant of the dynamic stiffness method (DSM) presented in reference [12]: essentially, the DSM is used to derive the dynamic stiffness matrix of the stiffened panel, and this is then coupled to two semi-infinite plate elements which carry the incident, reflected and transmitted waves (see Figure 2). Details of only the semi-infinite plate elements and the overall wave transmission calculation procedure are given in what follows, as full details of the dynamic stiffness analysis of the stiffened panel are available in reference [12].

The equation of motion which governs the linear, isotropic bending behaviour of the jth ($j = 1, 2$) semi-infinite plate may be written as

$$D_j \nabla^4 w + \rho_j \ddot{w} = 0, \tag{10}$$

where w is the out-of-plane displacement and D_j and ρ_j are the flexural rigidity and mass per unit area of the jth plate. The elastic tractions (shear S and bending moment M) on the edge which is attached to the stiffened panel ($y = 0$, see Figure 2) may be written in the forms [12]:

$$S = -D_j \left(\frac{\partial^3 w}{\partial y^3} + (2 - \sigma_j) \frac{\partial^3 w}{\partial y \, \partial x^2} \right), \qquad M = D_j \left(\frac{\partial^2 w}{\partial y^2} + \sigma_j \frac{\partial^2 w}{\partial x^2} \right), \tag{11, 12}$$

where σ_j is the Poisson ratio.

The fact that the plate is simply supported on the two longitudinal edges implies that the displacement can be expressed in terms of waves components of the form [12]

$$w = \alpha \sin (n\pi x/b) \, \mathrm{e}^{(\mathrm{i}\omega t + \mu_B y)}, \tag{13}$$

where n is the number of standing half-waves across the plate, α is a complex amplitude and μ_B is the appropriate exponent associated with a specified value of n. It follows from equation (10) that the admissible solutions for μ_B are given by

$$\mu_B^2 = (n\pi/b)^2 \pm k_b^2, \qquad k_b = (\rho_j \omega^2 / D_j)^{1/4}. \tag{14, 15}$$

Except for the presence of an incident wave, which will be introduced at a later stage in the analysis, the wave motion in each semi-infinite plate must either propagate towards infinity or decay in this direction. This implies that μ_B must be either positive real or positive imaginary for the left hand plate, and either negative real or negative imaginary for the right hand plate, thus allowing two valid solutions for μ_B to be identified for each plate. It then follows from equation (13) that the displacement and rotation of the junction line ($y = 0$) of either plate can be written as

$$\begin{bmatrix} w_e \\ \theta_e \end{bmatrix} = \begin{bmatrix} 1 & 1 \\ \mu_{B1} & \mu_{B2} \end{bmatrix} \begin{bmatrix} \alpha_{B1} \\ \alpha_{B2} \end{bmatrix} \sin \left(\frac{n\pi x}{b} \right) \mathrm{e}^{\mathrm{i}\omega t}, \tag{16}$$

where μ_{B1} and μ_{B2} are the two valid roots for plate in question, and α_{B1} and α_{B2} are the complex amplitudes of the two associated complementary functions. Similarly, equations (11) and (12) can be used to express the edge tractions in terms of α_{B1} and α_{B2}. By eliminating α_{B1} and α_{B2}, the following expression between the edge tractions and the displacements may be obtained:

$$\begin{bmatrix} S_e \\ M_e \end{bmatrix} = \frac{D_j}{\mu_{B1} - \mu_{B2}}$$

$$\times \begin{bmatrix} \mu_{B2} \mu_{B1}^3 - \mu_{B1} \mu_{B2}^3 & \mu_{B2}^3 - \mu_{B1}^3 + (2 - \sigma_j)(\mu_{B1} - \mu_{B2})(n\pi/b)^2 \\ \mu_{B2}^3 - \mu_{B1}^3 + (2 - \sigma_i)(\mu_{B1} - \mu_{B2})(n\pi/b)^2 & \mu_{B1}^2 - \mu_{B2}^2 \end{bmatrix}$$

$$\times \begin{bmatrix} w_e \\ \theta_e \end{bmatrix}. \tag{17}$$

The matrix that appears in this equation is the dynamic stiffness matrix of the semi-infinite plate. The dynamic stiffness matrix of the stiffened panel may be found by employing the analysis presented in reference [12]. With this approach, the panel is modelled as an assembly of plate elements, and to this end a node is introduced at each plate/stiffener junction. The stiffeners may either by modelled by using Euler–Bernoulli beam theory, or a fully dynamic model may be developed by using plate elements to model the behaviour of the flanges and webs. The net outcome of the stiffened panel model is a Q-degree-of-freedom dynamic stiffness matrix; degrees of freedom 1 and 2 are taken to represent the attachment to the left-hand semi-infinite plate, while degrees of freedom $Q-1$ and Q play the same role for the right-hand semi-infinite plate. The assembled dynamic stiffness equations for the complete structure (for a specified number of lateral half-wavelengths n) then have the form

$$\begin{bmatrix} D_{L11}+D_{E11} & D_{L12}+D_{E12} & \cdots & 0 & 0 \\ D_{L21}+D_{E21} & D_{L22}+D_{E22} & \cdots & 0 & 0 \\ \mathbf{0} & \mathbf{0} & \mathbf{D}_E & \mathbf{0} & \mathbf{0} \\ 0 & 0 & \cdots & D_{R11}+D_{E(Q-1)(Q-1)} & D_{R12}+D_{E(Q-1)Q} \\ 0 & 0 & \cdots & D_{R21}+D_{EQ(Q-1)} & D_{R22}+D_{EQQ} \end{bmatrix} \times \begin{bmatrix} w_{Le} \\ \theta_{Le} \\ \vdots \\ w_{Re} \\ \theta_{Re} \end{bmatrix} = \begin{bmatrix} S_{Le} \\ M_{Le} \\ \vdots \\ S_{Re} \\ M_{Re} \end{bmatrix}, \tag{18}$$

where the L and R subscripts represent the left and right semi-infinite plates and the E subscript represents the embedded stiffened panel. Equation (18) may be abbreviated in the form

$$\mathbf{D}\mathbf{b} = \mathbf{F}, \tag{19}$$

where $\mathbf{F}$ is the dynamic loading vector that arises from an incident wave of amplitude α_{inc} on the left-hand plate. All but the first two entries of this vector are zero and, following reference [5], the two non-zero entries, $\mathbf{F}_L$ say, can be written as

$$\mathbf{F}_L = \mathbf{D}_L\,\mathbf{b}'_L - \mathbf{F}'_L, \tag{20}$$

where $\mathbf{D}_L$ is the dynamic stiffness matrix of the left-hand plate. The entries of the vectors $\mathbf{b}'_L = (w'_e \;\; \theta'_e)^{\mathrm{T}}$ and $\mathbf{F}'_L = (S'M')^{\mathrm{T}}$ have the form

$$w'_e = \alpha_{inc}, \qquad \theta'_e = \mu\alpha_{inc}, \tag{21, 22}$$

$$S' = -\alpha_{inc}\,D_j(\mu^3 - (2-\sigma_j)\,(n\pi/b)^2\mu), \qquad M' = \alpha_{inc}\,D_j\,(\mu^2 - (n\pi/b)^2\sigma_j), \tag{23, 24}$$

where μ is the negative imaginary root yielded by equation (14).

Equation (19) can be solved to yield the degrees of freedom w_e and θ_e for each semi-infinite plate which can then be substituted into equation (16) to provide the complex amplitudes of the transmitted and reflected waves (α_t and α_r, say) for the specified number of transverse half-waves, n. The transmission and reflection coefficients are then defined as $\tau = |\alpha_t\,/\alpha_{\text{inc}}\,|^2$ and $\rho = |\alpha_r\,/\alpha_{inc}\,|^2$.

The transmission and absorption coefficients required in equations (8) and (9) are those associated with a diffuse incident wavefield. As described in section 2, the diffuse transmission and reflection coefficients are defined as

$$\langle \tau(\omega) \rangle = \tfrac{1}{2} \int_0^{\pi} \tau(\omega, \phi) \sin \phi \, \mathrm{d}\phi, \qquad \langle \rho(\omega) \rangle = \tfrac{1}{2} \int_0^{\pi} \rho(\omega, \phi) \sin \phi \, \mathrm{d}\phi, \quad (25, 26)$$

where ϕ is the angle between the incident wave heading and the junction line ($\theta = \pi/2 - \phi$ in equations (2) and (3)). In the present case $\tau(\omega, \phi)$ does not vary continuously over the range of ϕ, but discretely with integer values of n. The relationship between ϕ and n is

$$\phi = \cos^{-1}(n\pi/bk_b). \quad (27)$$

The diffuse transmission and reflection coefficients, at frequency ω, can then be evaluated by averaging τ and α over and the appropriate range of values of n. The absorption coefficient then follows from the relation

$$\langle \alpha \rangle = 1{\cdot}0 - \langle \tau \rangle - \langle \rho \rangle. \quad (28)$$

This procedure can be used to calculate the transmission and absorption coefficients for any panel or single joint which can be modelled by using the dynamic stiffness method.

An alternative to the present method of calculating $\langle \tau \rangle$ and $\langle \alpha \rangle$ might be envisaged in which the structure is idealized to be of infinite extent in the direction of the stiffeners. With this approach, equation (27) is not constrained to integer values of n, and incident waves of all headings can be considered. Although such an approach is routinely adopted in calculating the diffuse field transmission coefficients of a single joint, the method is not appropriate in the present case, since the detailed pass band/stop band behaviour of the system is crucially affected by the finite width of the panel.

3.2. APPROXIMATE CALCULATION

The calculation procedure described in the previous section leads to exact results for the transmission and absorption coefficients of the M-bay stiffened panel which is shown in Figure 2. A more approximate approach that requires significantly less computational effort is described in the present section; this approach is based on the general analysis of a one-dimensional waveguide which is presented in reference [8], and it leads to closed form approximate results for the transmission and absorption coefficients associated with each Fourier component n in equation (13).

Initially, it can be noted that for each Fourier component n the system shown in Figure 2 forms a one-dimensional waveguide, for which the wavenumbers in each panel are given by the solutions of equation (14). By assuming that any evanescent wave components affect the panel response only in the immediate vicinity of the stiffeners, the response of the panel can be approximated by a pair of propagating waves so that

$$w_m(y, t) = a_m \, \mathrm{e}^{\mathrm{i}k(L-y)} + b_m \, \mathrm{e}^{-\mathrm{i}k(L-y)}, \quad (29)$$

where a_m and b_m are, respectively, the amplitudes of the right- and left-going waves in panel m, as shown schematically in Figure 3. The wavenumber k which appears in equation (29) is the appropriate solution μ_B of equation (14) for the particular Fourier component n under investigation.

The waveguide joints (i.e., stiffeners) that are shown in Figure 3 are described here in terms of the wave transmission coefficient T and the reflection coefficients for right- and left-travelling waves, R^+ and R^- say. For the particular value of n under consideration, these coefficients can be found by making use of the method presented in section 3.1, or

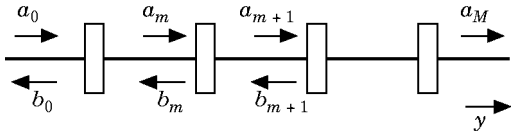

Figure 3. A schematic of the one-dimensional waveguide.

by using previously published methods [5]. If the stiffeners are undamped, then the transmission and reflection coefficients can be written in the form [15]

$$T = t\,\mathrm{e}^{\mathrm{i}\phi_t}, \qquad R^+ = r\,\mathrm{e}^{\mathrm{i}\phi_t + \mathrm{i}\phi_r + \phi} = R^-\,\mathrm{e}^{2\mathrm{i}\phi^\tau}, \qquad t^2 + r^2 = 1, \tag{30–32}$$

where t and r are the amplitudes of the coefficients and $\phi = \pm\pi/2$. With this notation, the wave components in bay $m+1$ can be related to those in bay m as follows:

$$\begin{pmatrix} a_{m+1} \\ b_{m+1} \end{pmatrix} = \begin{pmatrix} (1/t)\,\mathrm{e}^{-\mathrm{i}kL + \mathrm{i}\phi_t} & -(r/t)\,\mathrm{e}^{-\mathrm{i}kL - \mathrm{i}\phi_t - \mathrm{i}\phi} \\ -(r/t)\,\mathrm{e}^{\mathrm{i}kL + \mathrm{i}\phi_t + \mathrm{i}\phi} & (1/t)\,\mathrm{e}^{\mathrm{i}kL - \mathrm{i}\phi_t} \end{pmatrix} \begin{pmatrix} a_m \\ b_m \end{pmatrix}. \tag{33}$$

Free wave motion in an infinite periodic structure can be analyzed by employing Bloch's theorem [16], which in the present context states that $a_{m+1} = \lambda a_m$ and $b_{m+1} = \lambda b_m$, where λ is constant throughout the structure. In structural dynamics, this constant is normally expressed in the form $\lambda = \exp(-\mathrm{i}\varepsilon - \delta)$, where ε and δ are known, respectively, as the phase and attenuation constants. It follows by definition that λ is an eigenvalue of the matrix which appears in equation (33), and the associated characteristic equation can readily be shown to take the form

$$\lambda^2 - (2\lambda/t)\cos(kL - \phi_t) + 1 = 0 \Rightarrow \cos(\varepsilon - \mathrm{i}\delta) = (1/t)\cos(kL - \phi_t). \tag{34}$$

The solutions of this equation are of the type $(\lambda, 1/\lambda)$, corresponding to right-going and left-going wave motion. Here, "right-going" is taken to mean that the wave motion is associated with a net flow of energy to the right; i.e., $|a_m| > |b_m|$. With this convention the eigenvectors $(a_m\ b_m)$ associated with these two solutions can be written as $(1\ \alpha_1)$ and $(\alpha_2\ 1)$ where $|\alpha_i| \leqslant 1$; it then follows from equation (33) that

$$\alpha_1 = \mathrm{e}^{\mathrm{i}kL}(T/R^+)^*(\mathrm{e}^{-\mathrm{i}kL}/T^* - \lambda), \qquad \alpha_2 = \mathrm{e}^{-\mathrm{i}kL}(T/R^+)\,(\mathrm{e}^{\mathrm{i}kL}/T - 1/\lambda). \tag{35, 36}$$

The wave motion within the periodic system can be described in terms of a right-going and a left-going "periodic" wave—the wave motion at the left-hand side of the system (see Figure 3) will be made up of some combination of these two waves, so that it is possible to write

$$\begin{pmatrix} a_0 \\ b_0 \end{pmatrix} = A \begin{pmatrix} 1 \\ \alpha_1 \end{pmatrix} + B \begin{pmatrix} \alpha_2 \\ 1 \end{pmatrix}, \tag{37}$$

where A and B are complex constants. It then follows from Bloch's theorem that the wave motion at the right-hand side of the system must have the form

$$\begin{pmatrix} a_M \\ b_M \end{pmatrix} = A\lambda^M \begin{pmatrix} 1 \\ \alpha_1 \end{pmatrix} + B\lambda^{-M} \begin{pmatrix} \alpha_2 \\ 1 \end{pmatrix}. \tag{38}$$

If the wave motion is caused solely by an incident wave a_0 which impinges on the left-hand side of the system, then it follows on physical grounds that $b_M = 0$, from which it can be deduced that $B = -A\alpha_1\,\lambda^{2M}$. The wave components a_0, b_0 and a_M can then all

be expressed in terms of the single complex constant A, and the transmission and reflection coefficients of the system can be written as

$$\tau_M = \left|\frac{a_M}{a_0}\right|^2 = |\lambda^{2M}|\left(\frac{|1-\alpha_1\,\alpha_2\,|^2}{|1-\alpha_1\,\alpha_2\,\lambda^{2M}|^2}\right), \qquad \rho_M = \left|\frac{b_0}{a_0}\right|^2 = |\alpha_1\,|^2\left(\frac{|1-\lambda^{2M}|^2}{|1-\alpha_1\,\alpha_2\,\lambda^{2M}|^2}\right). \quad (39, 40)$$

The behaviour of the coefficients τ_M and ρ_M over a frequency band depends strongly on whether the frequency band of interest lies within a pass band or a stop band. Within a pass band, it can be noted that the coefficients display a rapid variation with frequency due to the presence of the term $\lambda^{2M} = \mathrm{e}^{-2\mathrm{i}M\varepsilon - 2\delta M}$ in equations (39) and (40), and a slower variation due to the frequency dependency of α_1 and $\alpha_1\,\alpha_2$. As discussed in reference [8], τ_M and ρ_M can be locally "smoothed" by averaging over a cycle of $\mathrm{e}^{-2\mathrm{i}\varepsilon M}$ on the assumption that α_1 and $\alpha_1\,\alpha_2$ remain approximately constant. This approach yields

$$\bar{\tau}_M = \frac{\mathrm{e}^{-2\delta}|1-\alpha_1\,\alpha_2\,|^2}{1-|\alpha_1\,\alpha_2\,|^2\,\mathrm{e}^{-4\delta M}}, \quad (41)$$

$$\bar{\rho}_M = |\alpha_1\,|^2\left(\frac{1-\alpha_1\,\alpha_2\,(1+\mathrm{e}^{-4M\delta}) + Z^2 - (Z^4-4Z^2+1)^{1/2}}{\alpha_1\,\alpha_2\,(Z^4-4Z^2+1)^{1/2}}\right), \quad (42)$$

where $Z = \alpha_1\,\alpha_2\,\mathrm{e}^{-2M\delta}$. Equation (41) was first derived in reference [8], and this result has been extended here by considering also the smoothed reflection coefficient, equation (42). To facilitate the evaluation of equations (41) and (42) it can be shown that

$$\alpha_1\,\alpha_2 = 1 + (2/r^2)\,(t^2\sin^2(\varepsilon - \mathrm{i}\delta) - t\sin(\varepsilon - \mathrm{i}\delta)\sqrt{1 - t^2\cos^2(\varepsilon - \mathrm{i}\,\delta)}). \quad (43)$$

and also from equations (34) and (35) that

$$|\alpha_1\,|^2 = (1/r^2)\,(1 + t^2\,\mathrm{e}^{-2\delta} - 2t\,\mathrm{e}^{-\delta}\cos(kL - \phi_t - \varepsilon)). \quad (44)$$

Equations (43) and (44) enable the smoothed reflection and transmission coefficients of the stiffened panel to be expressed in terms of the propagation constants δ and ε, and the transmission properties r, t and ϕ_t of a single stiffener.

In principle, the band-averaged transmission and reflection coefficients can be obtained by integrating τ_M and ρ_M over the appropriate wavenumber range, although in practice this will generally have to be done numerically. A more approximate approach is to assume that within a stop band $\tau_M = 0$ and $\rho_M = 1$, while within a pass band τ_M and ρ_M are constant and equal to the *mid-band* value (i.e., the value at $\varepsilon = \pi/2$). In this regard, it can be noted that the value of the mid-band attenuation constant, δ_{mid}, is given by [8]

$$\delta_{mid} = \sinh^{-1}[(1/t)\sinh(\pi M_0\,/2)], \quad (45)$$

where $M_0 = \omega\eta v$ is the modal overlap factor for a single bay of the system; here η is the loss factor and $v = (L/\pi c_g)$ (group velocity $c_g = \partial\omega/\partial k$) is the modal density of the bay.

Within the current analysis framework, the coefficients τ_M and ρ_M must be evaluated for all propagating values of transverse wavenumber n and integrated as described in the previous section to yield the diffuse transmission and reflection coefficients. These may then be used to evaluate the absorption coefficient of the periodic system under the action of an incident diffuse wavefield. Finally, the diffuse field power transmission and absorption coefficients derived in this way can be substituted into equations (8) and (9) to yield the coupling loss factors and loss factor of the embedded periodic coupling.

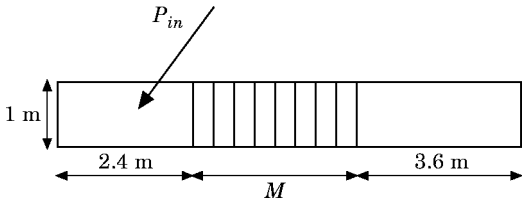

Figure 4. The planform of the example structures.

4. NUMERICAL EXAMPLES

The foregoing theory has been applied to two example stiffened panel systems; in each case the stiffened panel consists of an eight bay (nine stiffener) periodic system which forms the coupling between two rectangular unstiffened panels. The planform geometry of each system is shown in Figure 4: the whole structure is of width 1 m and the two unstiffened plates are of length 2·4 m and 3·6 m. Each has a thickness of 2 mm. The distinguishing feature between the two example systems lies in the geometry of the stiffeners, and the two arrangements considered are detailed in Figure 5. In each case the material is taken to be aluminium with $E = 70$ GPa, $\rho_{vol} = 2700\ \mathrm{Kgm}^{-3}$ and $\sigma = 0{\cdot}3$. The two systems are designed such that system 1 has light stiffeners, giving a strongly coupled periodic system, while system 2 has moderate stiffeners, giving a much more weakly coupled periodic system. In computing the majority of the results which are presented, the stiffeners have been modelled by using Euler–Bernoulli beam theory. This allows the present method to be compared with existing SEA and wave intensity analysis (WIA) codes in the absence of the complicating effects of the stiffener dynamics, which can arise in deep stiffeners at higher frequencies [17]. By consistently modelling the stiffeners as beams, the significance of the assumptions adopted in each of the methods can be assessed for the example structures. The effect of the dynamics of the stiffener is investigated briefly towards the end of the present section by using the dynamic stiffness method to model the stiffeners as fully dynamic plate assemblies.

Example propagation constants ε and δ for the periodically stiffened panel employed in system 1 are shown in Figure 6(a) for the case of zero damping ($\eta = 0$); the results concern only the first Fourier component of the motion ($n = 1$) and the upper frequency is limited to 190 Hz. Three pass bands (in which $\delta = 0$) are discernible in Figure 6(a), and it can be expected that vibration transmission through a finite stiffened panel will be concentrated within these bands. This is confirmed by Figure 6(b), in which the

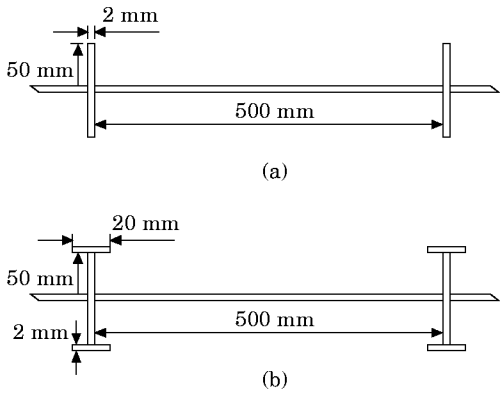

Figure 5. The geometries of the example stiffened structures. (a) System 1; (b) system 2.

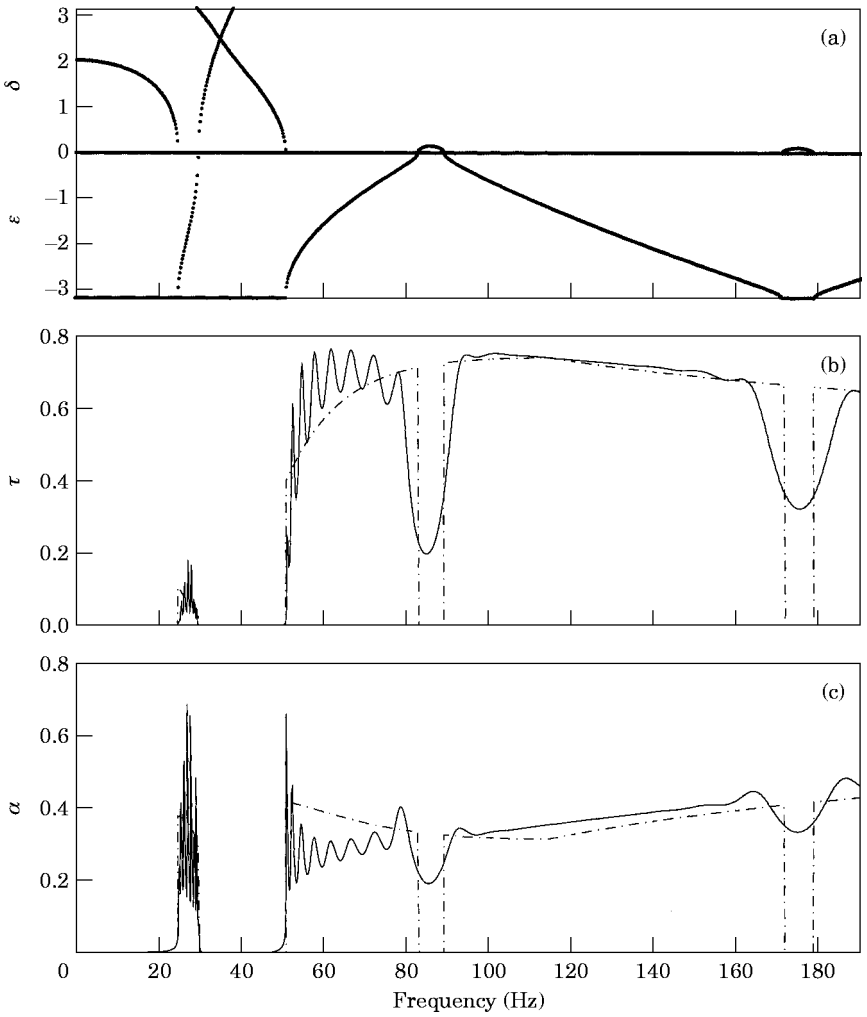

Figure 6. System 1: propagation constants (a), transmission coefficients (b) and absorption coefficients (c) for $n = 1$. ·–·–, Approximate; ——, exact.

transmission coefficient of the eight-bay panel is shown for the case $\eta = 0{\cdot}01$. The "exact" results yielded by the analysis presented in section 3.1 display eight peaks per pass band; were the panel undamped then the transmission coefficient would achieve unity at each of these peaks [8]. The approximate results yielded by the analysis presented in section 3.2 provide a good estimate of the average transmission coefficient in each pass band, and a similar level of agreement is shown in Figure 6(c) for the absorption coefficient.

The results shown in Figure 6 relate only to the $n = 1$ Fourier component. Results for all relevant values of n over an extended frequency range are shown in Figure 7, where it can be seen that a complex system of overlapping pass bands occurs. The agreement between the exact and the approximate values of the transmission and absorption coefficients is generally good. It has been found that the response predictions are not sensitive to the value of the absorption coefficient for the present structure, since the absorption tends to make less than a 20% difference to the internal loss factor via equation (9).

Results for the response of the structure (system 1) to rain-on-the-roof forcing of the left-hand plate are shown in Figure 8. The results are presented in terms of a dB energy level difference between the two endplates, i.e., $10 \log (E_2 / E_1)$, and five sets of results are shown as follows: (i) benchmark exact results computed by applying the dynamic stiffness method [12] to the complete system; (ii) standard SEA results obtained by treating each bay of the stiffened panel as a separate subsystem; (iii) wave intensity analysis (WIA) results in which the SEA diffuse wavefield assumption is relaxed; (iv) results yielded by the present two-subsystem model with exact transmission and absorption coefficients; and (v) results yielded by the present method with approximate transmission and absorption coefficients.

In considering the standard SEA results shown in Figure 8, it can be recalled that the method is based on the assumptions that (a) the wavefield in each subsystem is diffuse and (b) all wave components are uncorrelated. Assumption (a) is in error for the present

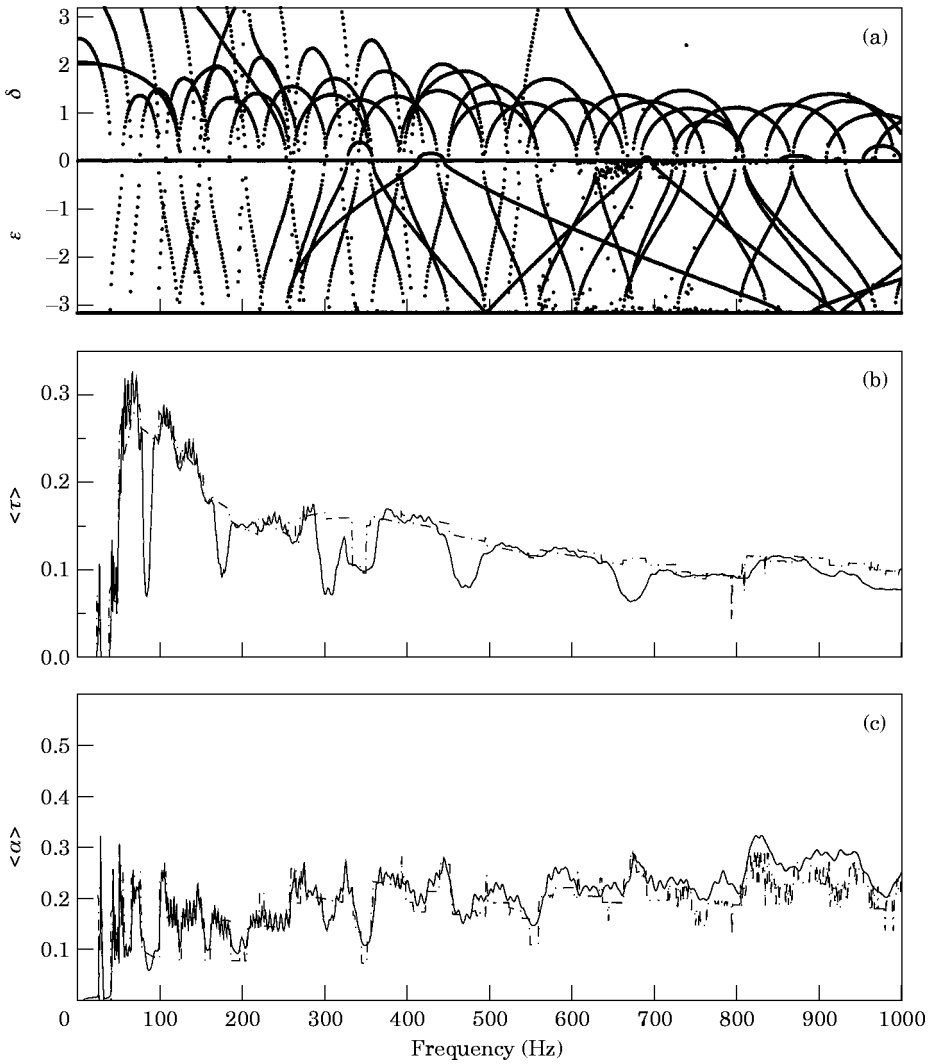

Figure 7. System 1: propagation constants (a), transmission coefficients (b) and absorption coefficients for all valid n. ·–·–, Approximate; ——, exact.

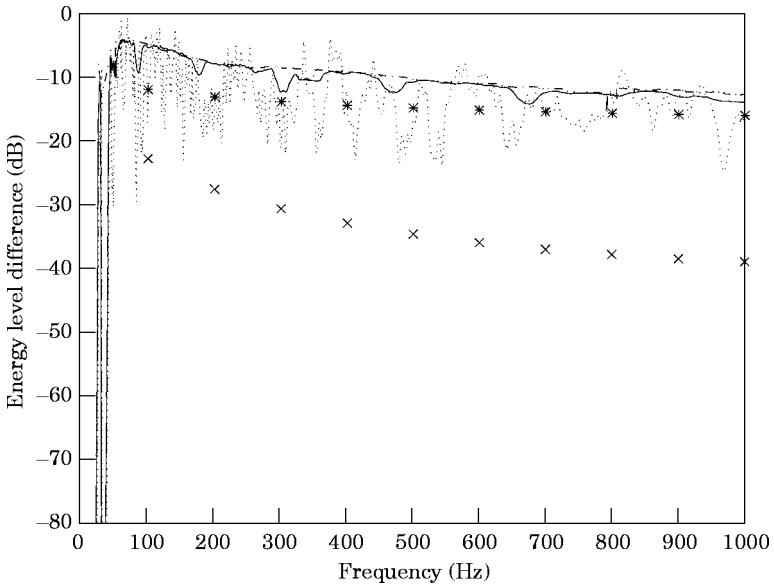

Figure 8. System 1: comparison of methods. ····, Exact (dynamic stiffness method); ×, classical SEA; *, WIA, 50 Fourier components; ·–·–, SEA with approximate coupling ——, SEA with exact coupling.

structure, since the stiffeners act as spatial filters which favour the waves near to normal incidence. This assumption is relaxed in WIA [13], where the angular distribution of the wavefield in each subsystem is expanded in terms of a Fourier series—this leads to much improved results, as shown in Figure 8, although for the present example 50 Fourier components were needed to ensure converged results at the higher frequencies. Assumption (b) regarding the phase of the various wave components is also adopted in WIA, and this leads to differences of the order of 3 dB between WIA and the exact results.

The present approach to modelling the system as two SEA subsystems incorporates a detailed model of the stiffened panel behaviour, and thus wave filtering and phase effects are both captured, as evidenced by the good agreement with the exact results shown in Figure 8. It can be seen that the use of the approximate formulae for the transmission and absorption coefficients does not lead to a significant loss in the accuracy of the prediction.

The propagation constants ε and δ associated with the stiffened panel employed in system 2 are shown in Figure 9(a) for the case of $\eta = 0$ and $n = 1$. The fact that the system 2 stiffeners are of a heavier gauge than those of system 1 leads to a more weakly coupled periodic structure which displays narrower pass bands, as revealed by a comparison of Figures 6 and 9. The fact that the pass bands are narrower reduces the tendency for the bands associated with the different values of n to overlap and, as shown in Figure 10(a–c), this produces transmission and absorption coefficients which are highly frequency dependent. This leads to a very noticeable irregularity in the forced response results which are shown in Figure 11, with a very sharp response trough occurring in the vicinity of 900 Hz. Neither standard SEA nor WIA is able to predict this behaviour: WIA yields poor results beyond 700 Hz whereas standard SEA gives a poor prediction over the whole frequency range. As in the case of system 1, the present modified SEA approach yields a good response prediction which captures the phase related pass band/stop band nature of the system dynamics. Again, the results obtained by using the approximate, rather than exact, values of the absorption and transmission coefficients do not display any marked loss in accuracy.

There has been much recent interest in the effect of structural disorder on the behaviour of a periodic system (see, for example, references [18–20]). Specifically, it has been shown that relatively small levels of disorder can have a marked effect on the pass band/stop band behaviour of the system—high levels of attenuation can be produced within a pass band ("vibration localization"), and conversely increased vibration transmission can occur within a stop band. The present analysis procedure is based on the assumption of "perfect" periodic structure behaviour, and it is therefore relevant to investigate the sensitivity of the response of the systems considered here to structural disorder. To this end, system 2 has been randomized by introducing variability into the length of each bay of the stiffened panel: the length of the nth bay is changed by an amount Z_n, where Z_n is chosen from a uniform distribution with $-(X/100)L < Z_n < (X/100)L$, where L is the nominal bay length and X is a disorder parameter, so that the system is said to have $X\%$ disorder. Results for the response of the disordered system are presented in Figure 12 for the case $X = 10\%$; the results from 20 realizations (i.e., 20 different random systems) are shown, together with the ensemble average response. It is clear that the system is particularly

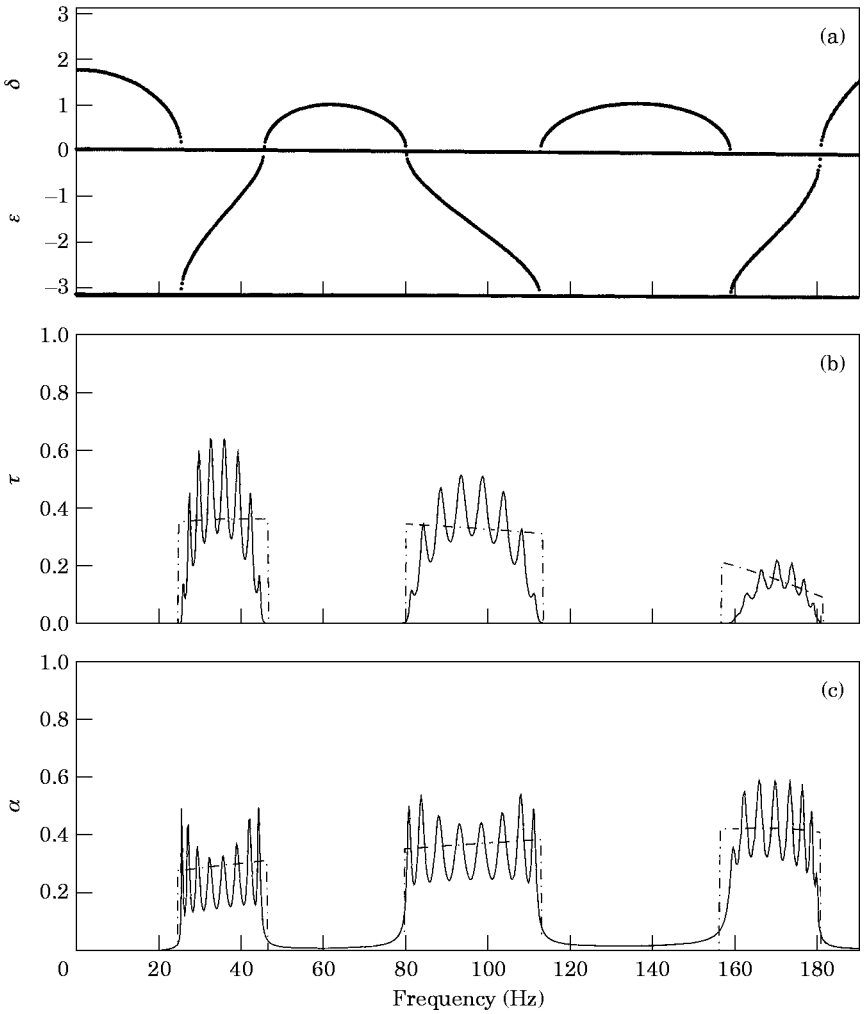

Figure 9. System 2: propagation constants (a), transmission coefficients (b) and absorption coefficients (c) for $n = 1$. ·–·–, Approximate; ——, exact.

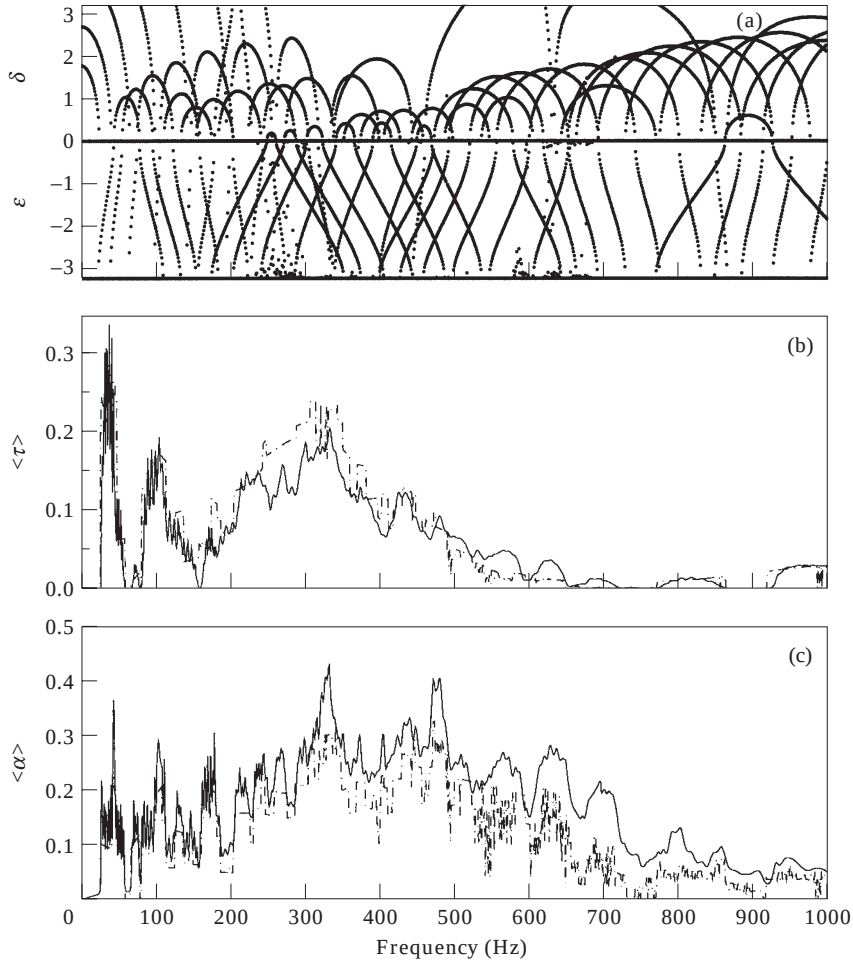

Figure 10. System 2: propagation constants (a), transmission coefficients (b) and absorption coefficients (c) for all valid n. ·—·–, Approximate; ——, exact.

sensitive to the effects of disorder in the range 700–900 Hz. This is also found to be the case for other levels of disorder ($X = 1\%$, 5%, 10% and 30%), as shown in Figure 13. This can be explained by referring to Figure 11, where it can be seen that the results yielded by WIA for this system are reasonably accurate up to 700 Hz and reasonably inaccurate beyond 700 Hz; this implies that phase effects (which are neglected in WIA) are very significant beyond 700 Hz and it is therefore to be expected that the system will be sensitive to disorder in this region—disorder in the bay length modifies the phase change in a wave as it propagates from one stiffener to the next. The levels of disorder considered in Figure 13 are relatively high and certainly beyond normal manufacturing tolerances—once the disorder falls to $X = 1\%$, the present analysis method, based on ideal periodic structure behaviour, yields a good estimate of the system response across the whole frequency range.

As mentioned earlier in this section, it has previously been shown that "internal" stiffener dynamics can in some cases have a significant effect on the behaviour of a periodically stiffened system [17]. These effects have not been considered here, since Euler–Bernoulli beam theory has been used to model the stiffeners—this has been done consistently, both in the dynamic stiffness forced response analysis and in the computation

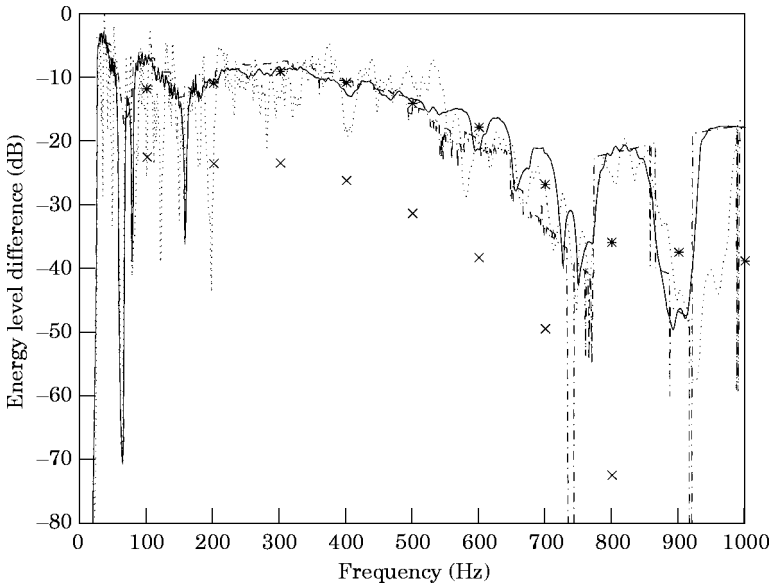

Figure 11. System 2: comparison of methods. Key as Figure 8.

of the transmission and absorption coefficients of the stiffened panel. By using the dynamic stiffness method [12], it is in fact possible to compute the response of the system with full account taken of stiffener dynamics by modelling each stiffener as an assembly of plate elements. Results obtained in this way are compared with the previous "beam model" in Figures 14 and 15. Clearly, stiffener dynamic effects have little influence on the response of system 1, although there is a marked change in the response of system 2. In the latter case, the response shows a more clearly distinguishable pass band/stop structure, and this

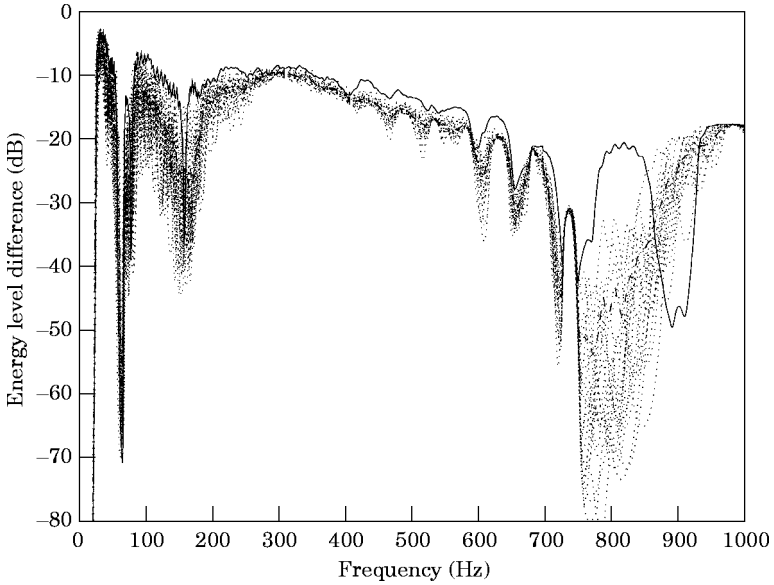

Figure 12. The effect of 10% disorder on system 2. ——, Ideal panel; ·–·–, emsemble average; ····, 20 disordered runs.

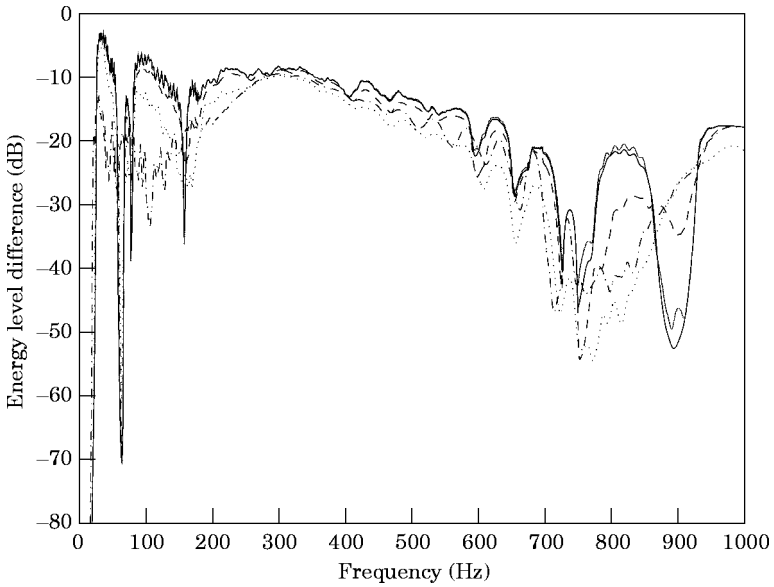

Figure 13. The effect of disorder on system 2. ——, Ordered ——, 1%; – –, 5%; ····, 10%; ·–·–, 30%.

would be captured by the present method provided that stiffener dynamics were fully considered in the calculation of the band averaged transmission and absorption coefficients. This can be achieved by including stiffener dynamics in the matrix $\mathbf{D}_E$ which appears in equation (17), or by extending the analysis contained in reference [5] to the case of full stiffener dynamics (as recently performed by Heron [21]).

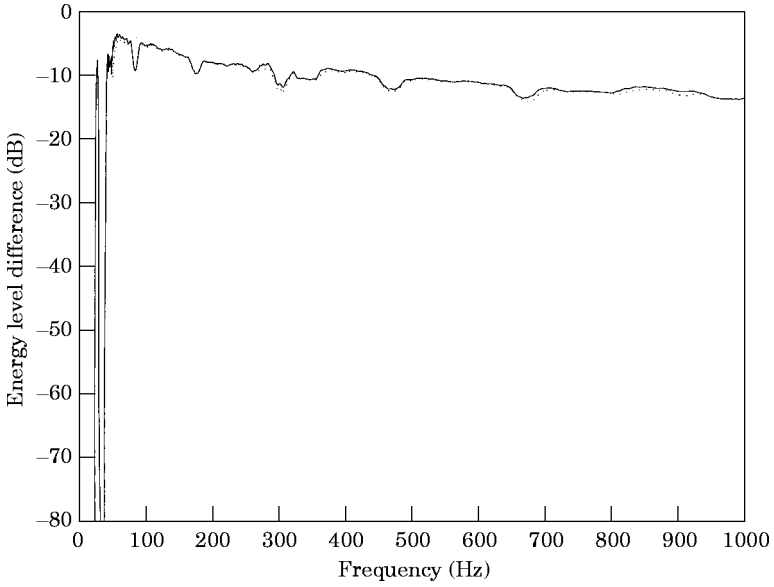

Figure 14. System 1: comparison of stiffener model. ····, Beam stiffeners; ——, dynamic stiffeners.

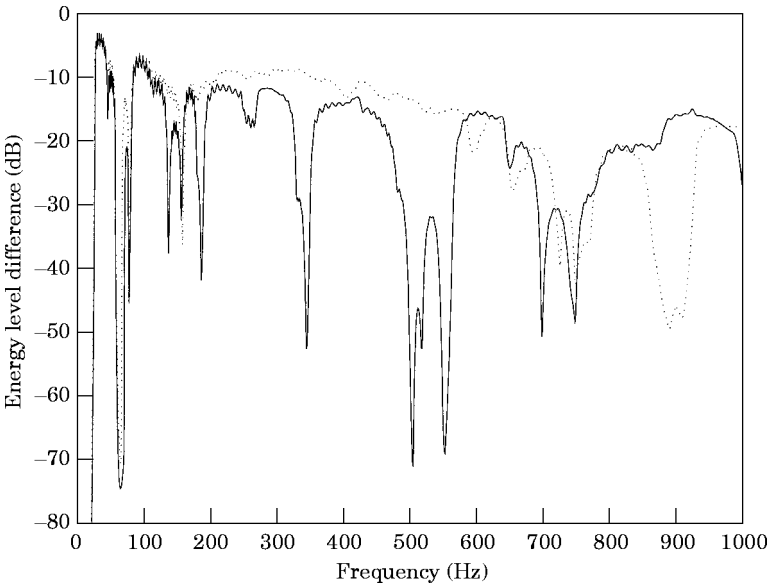

Figure 15. System 2: comparison of stiffener model. Key as Figure 14.

5. CONCLUSIONS

This work has been concerned with how a stiffened panel might be modelled within the context of Statistical Energy Analysis. It has been suggested that such a panel might be modelled as a damped coupling element the transmission and absorption coefficients of which are calculated on the basis of periodic structure theory. In this regard it has been shown that the diffuse field transmission and absorption coefficients can be estimated to an acceptable degree of accuracy by considering the transmission properties of a single stiffener and employing the theory developed in reference [8]. The main advantage of the proposed method is that the pass band/stop band behaviour of the periodically stiffened panel is encapsulated within the absorption and transmission coefficients, so that the response predictions yielded by the method incorporate these effects. This compares with a standard SEA approach in which all phase effects are averaged, so that periodic structure effects cannot readily be modelled. For the type of structure considered here, wave-intensity analysis (WIA) offers considerable improvement over standard SEA by allowing for the presence of non-diffuse wavefields, although again, phase effects and pass band/stop band behaviour cannot be captured.

The present study has indicated that the "damped coupling" approach to modelling a stiffened panel is certainly a feasible and accurate technique for the type of structure considered here; further work is needed to consider *in situ* panels in more complex structural geometries, and efficient means of employing the approach in a large-scale SEA response predictions will need to be developed.

ACKNOWLEDGMENTS

The present work has been funded by the EPSRC through the Marine Technology Directorate under contract number C41R201. The authors gratefully acknowledge the help of Dr F. M. Khumbah for providing the WIA software used in this study.

REFERENCES

1. R. H. Lyon and R. G. DeJong 1995 *Theory and Application of Statistical Energy Analysis* (second edition). Boston: Butterworth–Heinemann.
2. F. J. Fahy 1994 *Philosophical Transactions of the Royal Society* **346**, 431–447. Statistical energy analysis: a critical overview.
3. R. S. Langley 1989 *Journal of Sound and Vibration* **135**, 499–508. A general derivation of the statistical energy analysis equations for coupled dynamic systems.
4. E. C. N. Wester and B. R. Mace 1996 *Journal of Sound and Vibration* **193**, 793–822. Statistical energy analysis of two edge-coupled rectangular plates: ensemble averages.
5. R. S. Langley and K. H. Heron 1990 *Journal of Sound and Vibration* **143**, 241–253. Elastic wave transmission through plate/beam junctions.
6. K. H. Heron 1996 ISMA 21, *Noise and Vibration Engineering Conference*, *Leuven*, *Belgium*. Predictive statistical energy analysis using the wave approach.
7. A. J. Keane and W. G. Price 1989 *Proceedings of the Royal Society of London* **A423**, 331–360. Statistical energy analysis of periodic structures.
8. R. S. Langley 1996 *Journal of the Acoustical Society of America* **100**, 304–311. The frequency band-averaged wave transmission coefficient of a periodic structure.
9. J. C. Sun, N. Lalor and E. J. Richards 1987 *Journal of Sound and Vibration* **112**, 321–330. Power flow and energy balance of non-conservatively coupled structures, I: theory.
10. F. J. Fahy and Y. De-Yuan 1987 *Journal of Sound and Vibration* **114**, 1–11. Power flow between non-conservatively coupled oscillators.
11. M. Beshara and A. J. Keane 1996 *Journal of Sound and Vibration* **198**, 95–122. Statistical Energy Analysis of multiple, non-conservatively coupled systems.
12. R. S. Langley 1992 *Journal of Sound and Vibration* **156**, 521–540. A dynamic stiffness technique for the vibration analysis of stiffened shell structures.
13. R. S. Langley 1992 *Journal of Sound and Vibration* **156**, 521–540. A wave intensity technique for the analysis of high frequency vibration.
14. R. J. M. Craik 1996 *Sound Transmission Through Buildings using Statistical Energy Analysis*. Aldershot: Gower.
15. B. R. Mace 1992 *Journal of Sound and Vibration* **155**, 375–381. Reciprocity, conservation of energy and some properties of reflection and transmission coefficients.
16. L. Brillouin 1946 *Wave Propagation in Periodic Structures*. New York: Dover.
17. C. H. Hodges, J. Power and J. Woodhouse 1985 *Journal of Sound and Vibration* **101**, 219–235. The low frequency vibration of a ribbed cylinder, part I: theory.
18. C. Pierre 1990 *Journal of Sound and Vibration* **139**, 111–132. Weak and strong vibrational localization in disordered structures: a statistical investigation.
19. C. H. Hodges and J. Woodhouse 1983 *Journal of the Acoustical Society of America* **74**, 894–905. Vibration isolation from irregularity in a near periodic structure: theory and measurements.
20. R. S. Langley 1995 *Journal of Sound and Vibration* **188**, 717–743. Wave transmission through one-dimensional near-periodic structures: optimum and random disorder.
21. K. H. Heron 1995 *Statistical Energy Analysis*: *Strip Plate Theory*. CEC IMT Area3 RHINO RH8DRA039(A)T/D34.